Am J Cancer Res 2024;14(3):1121-1138
www.ajcr.us /ISSN:2156-6976/ajcr0153362

Original Article

Endogenous S100P-mediated autophagy regulates the chemosensitivity of leukemia cells through the p53/AMPK/mTOR pathway

Min Peng[1], Fanghua Ye[1], Chenying Fan[1], Jiajia Dong[1], Wenwen Chai[2], Wenjun Deng[1], Hui Zhang[1], Liangchun Yang[1]

[1]Department of Pediatrics, Xiangya Hospital Central South University, Changsha 410008, Hunan, The People's Republic of China; [2]Department of Nuclear Medicine, Hunan Cancer Hospital/The Affiliated Cancer Hospital of Xiangya School of Medicine, Central South University, Changsha 410008, Hunan, The People's Republic of China

Received September 10, 2023; Accepted March 2, 2024; Epub March 15, 2024; Published March 30, 2024

Abstract: Autophagy, a highly regulated lysosome-dependent catabolic pathway, has garnered increasing attention because of its role in leukemia resistance. Among the S100 family of small calcium-binding proteins, S100P is differentially expressed in various tumor cell lines, thereby influencing tumor occurrence, invasion, metastasis, and drug resistance. However, the relationship between S100P and autophagy in determining chemosensitivity in leukemia cells remains unexplored. Our investigation revealed a negative correlation between S100P expression and the clinical status in childhood leukemia, with its presence observed in HL-60 and Jurkat cell lines. Suppression of S100P expression resulted in increased cell proliferation and decreased chemosensitivity in leukemia cells, whereas enhancement of S100P expression inhibited cell proliferation and increased chemosensitivity. Additionally, S100P knockdown drastically promoted autophagy, which was subsequently suppressed by S100P upregulation. Moreover, the p53/AMP-activated protein kinase (AMPK)/mammalian target of rapamycin (mTOR) pathway was found to be functionally associated with S100P-mediated autophagy. Knockdown of S100P expression led to a decrease in p53 and p-mTOR levels and an increase in p-AMPK expression, ultimately promoting autophagy. This effect was reversed by administration of Tenovin-6 (a p53 activator) and Compound C (an AMPK inhibitor). The findings of our in vivo experiments provide additional evidence supporting the aforementioned data. Specifically, S100P inhibition significantly enhanced the growth of HL-60 tumor xenografts and increased the expression of microtubule-associated protein 1 light chain 3 and p-AMPK in nude mice. Consequently, it can be concluded that S100P plays a regulatory role in the chemosensitivity of leukemia cells by modulating the p53/AMPK/mTOR pathway, which controls autophagy in leukemia cells.

Keywords: S100P, autophagy, leukemia, chemosensitivity, p53

Introduction

Acute leukemia (AL) is a neoplastic disorder characterized by the presence of undifferentiated hematopoietic stem cells. This condition can be further classified into acute myeloid leukemia (AML) and acute lymphoblastic leukemia (ALL). Among pediatric cases of AL, ALL accounts for approximately 80%, while AML represents 15-20%. Advancements in chemotherapy regimens and the introduction of more precise treatments have led to notable improvements in survival rates. Currently, the estimated survival rate for pediatric patients with ALL is approximately 90%, whereas the long-term survival rate for children with AML is 70% [1, 2]. However, some children continue to receive conventional chemotherapy, which leads to the development of chemoresistance and subsequent disease recurrence [3]. Furthermore, the prognosis of children experiencing refractory relapse is exceedingly poor, with a 5-year overall survival rate of less than 10% [4]. Accumulating evidence suggests a significant correlation between chemoresistance and reduced drug absorption, increased drug efflux, mutations in drug targets, and enhanced DNA damage repair capabilities [5-7]. However, the

https://doi.org/10.62347/NWXE8730

precise molecular mechanisms underlying drug resistance in AL are yet to be fully elucidated.

Autophagy is a cellular process involving the transfer of proteins and aging organelles into vesicles that merge with lysosomes to create autophagolysosomes for the digestion and degradation of ingested substances. Autophagy has been implicated in various human diseases, such as neurodegenerative diseases, cancer, and immune disorders [8-10]. Emerging evidence has suggested that altered autophagy is associated with these conditions. Autophagy plays a dual role in the development of cancer. On the one hand, it can impede tumor growth through autophagy-induced cell death. On the other hand, autophagy protects cancer cells from the detrimental effects of radiation therapy, chemotherapy, and nutrient deficiency during tumor development [10-12]. Numerous signaling pathways are believed to participate in the regulation of autophagy. Among these, the AMP-activated protein kinase (AMPK)/mammalian target of rapamycin (mTOR) has been acknowledged as a pivotal pathway in regulating autophagy [13, 14]. Our previous research showed that inhibiting mTOR activation can induce autophagy in leukemia cells, thereby promoting their survival [15]. Additionally, the induction of autophagy has been associated with survival response during chemotherapy, which diminishes treatment effectiveness [10, 11, 14]. Although autophagy plays a crucial role in pediatric AL chemoresistance, the precise mechanism remains unclear.

Human S100P is a calcium-binding protein belonging to the S100 protein family. It is located on chromosome 4 (chromosome 4p16). Similar to other S100 proteins, S100P possesses two consecutive EF-hands containing Ca^{2+} binding sites that play a role in various biological processes [16]. Additionally, S100P has both intracellular and extracellular functions [17, 18]. S100P interacts with the extracellular receptor for advanced glycation end products and engages in various intracellular associations, including ezrin-paladin and α7-integrin, promoting multiple cell survival pathways, proliferation, and invasion [17-19]. S100P expression correlates with drug resistance and metastasis in several other cancers, including colon, ovarian, breast, lung, nasopharyngeal, and cervical cancers [19, 20]. A growing body of evidence indicates that autophagy is a cellular survival mechanism in response to the stress induced by cancer treatment. In a previous study, we demonstrated that S100A8, a member of the calbindin S100 family, plays a crucial role as an autophagy-promoting protein that enhances leukemia cell survival and regulates drug resistance [21]. A previous report suggested that the efficacy of leukemia chemotherapy could be enhanced by the involvement of the S100 calcium-binding protein in autophagy. However, the mechanism by which S100P-mediated autophagy promotes chemoresistance in leukemia remains unclear.

This study demonstrates a negative correlation between S100P expression in pediatric AL and the clinical status of patients, specifically in primary bone marrow mononuclear cells (BMMCs) from patients with pediatric AL, as shown in this study. The study also reveals that the overexpression of S100P inhibits autophagy induced by Hank's Balanced Salt Solution (HBSS) and enhances the sensitivity of leukemia cells to chemotherapeutic drugs. Conversely, the downregulation of S100P expression by shRNA silencing resulted in the opposite effects. Additionally, our findings indicate a functional association between the p53/AMPK/mTOR pathway and S100P-induced autophagy and chemosensitivity. These findings support the notion that S100P could potentially be targeted for therapeutic interventions in leukemia treatment.

Materials and methods

Reagents and cell culture

3-Methyladenine (3-MA), Cytarabine (Ara-C), adriamycin (ADM), Tenovin-6, Compound C and lysosomal protease inhibitors E64d, pepstatin A [22] were purchased from GlpBio (Montclair, CA, USA); AML cell lines (MV4-11, THP-1, HL-60, KASUMI1) and ALL cell lines (NALM-6, MOLT4, Jurkat) from Xiangya School of Medicine Type Culture Collection (Changsha, China). All the cells were cultivated in RPMI-1640 medium (GIBCO, Gaithersburg, USA), and grown in a humidified incubator at 37°C with 5% CO_2 (Thermo Fisher Scientific Inc., USA).

Patients and specimen collection

The Hospital's Ethics Committee approved the study protocol, and all participants provided

written informed consent before the clinical samples were used. Based on May-Grunwald Giemsa-stained bone marrow smears and cytochemistry, AL was diagnosed using the French-American-British group criteria. Primary disease, complete remission (CR), refractory disease, and bone marrow relapse were defined per the National Cancer Institute guidelines. With informed consent, BMMCs were obtained from the bone marrow samples of pediatric patients with AL. In our study, we enrolled 45 patients with ALL (23 in the primary phase, 6 in relapse, and 16 in CR), 26 patients with AML (16 in the primary phase, 4 in relapse, and 6 in CR). Using Ficoll density gradient centrifugation, BMMCs were isolated. Patients were divided into median S100P low and high-expression groups based on BMMC mRNA levels in patients with primary AL. Diagnoses and risk stratification of ALL were based on the Chinese Children's Cancer Group study ALL-2015 (CCCG-ALL-2015) [23, 24], and diagnoses and risk stratification of AML were based on the Children's Cancer and Leukemia Group study AML-2015 (CCLG-AML-2015) [25].

RNA interference and lentivirus transfection

Lentiviruses expressing S100P and S100P short hairpin RNA (shRNA) were purchased from Shanghai GeneChem Co. According to the manufacturer's instructions, S100P shRNA lentiviral knockdown or control shRNA were packaged in an HIV-based packaging mix (GeneChem Inc.) to infect HL-60/Jurkat cells and promote the constitutive repression of S100P. HL-60/Jurkat cells were transduced with lentiviral particles encoding S100P-GFP or GFP alone. Stable clones were selected using puromycin. The shRNA sequences for S100P were as follows: S100P shRNA1: 5'-CCGGCTGTCACAAGTACTTTGAGAACTCGAGTTCTCAAAGTACTTGTGACAGTTTTTT-3'; S100P shRNA2: 5'-CCGGGCTCAAGGTGCTGATGGAGAACTCGAGTTCTCCATCAGCACCTTGAGCTTTTT-3'; S100P shRNA3: 5'-CCGGAATGGAGATGCCCAGGTGGACCTCGAGGTCCACCTGGGCATCTCCATTTTTTT-3'. Non-silencing shRNA (control shRNA) was used as mock-transfected controls (target sequence): 5'-TTCTCCGAACGTGTCACGT-3'. S100P expression was verified using qRT-PCR and western blotting. Two S100P shRNAs (S100P shRNA1 and S100P shRNA2) that proved to be the most effective for the knockdown of gene expression were selected.

Quantitative real-time polymerase chain reaction (qRT-PCR)

Total RNA was isolated from BMMCs and different cells using Trizol reagent following manufacturer's instructions and cDNA was synthesized according to the procedures described previously via PrimeScript™ RT master mix (Yeasen Biotech Co., Ltd., Shanghai, China). A 7900 Real-Time PCR System (Applied Biosystems, Foster City, CA) with Hieff® qPCR SYBR Green Master Mix (Low Rox Plus Yeasen Biotech Co., Ltd., Shanghai, China) was used to perform quantitative PCR (qPCR). To standard relative mRNA expression, the forward primer was constructed using 5'-CTGGAACGGTGAAGGTGACA-3', and reverse primer was constructed using 5'-CGGCCACATTGTGAACTTTG-3'. In our research, primers were used as follows: S100P forward 5'-GGAGATGCCCAGGTGGACTT-3' and reverse 5'-TACTTGTGACAGGCAGACGTGAT-3'. In terms of cycling conditions, 95°C for 5 min, followed by 40 cycles of 95°C for 10 sec, and 60°C for 30 sec. In triplicate, samples were examined with the 2-ΔΔCq [26] method to calculate relative gene expression.

Antibodies and western blot

Antibodies from the following companies were used in our study: rabbit anti-S100P (#A14780), rabbit anti-β-actin (#AC026), rabbit anti-Tubulin (#AC008), rabbit anti-Fibrillarin (#A13490), rabbit anti-LC3B (#A19665), rabbit anti-p62 (#A19700), rabbit anti-CDK2 (#A0094), rabbit anti-cyclinD1 (#A19038), rabbit anti-Bcl-2 (#A19693) were obtained from ABclonal (Wuhan, China); rabbit antibodies against phospho(p)-mTORS2448 (#AF3308), mTOR (#AF6308), p53 (#AF0879), p-AMPKαT172 (#AF3423), AMPKα (#AF6423), from Affinity Biosciences (Changzhou, China), horseradish peroxidase (HRP)-conjugated goat anti-rabbit IgG (#AS014) from ABclonal (Wuhan, China); After rinsing cells with PBS, they were collected and resuspended in lysis buffer (Beyotime, Beijing, China) for 15 minutes. They were then fractionated with the nuclear cytoplasm fraction kit (Beyotime, Beijing, China). Using BCA assay (Beyotime, Beijing, China) to measure the extracted protein concentrations. SDS-PAGE was used to resolve proteins and PVDF membranes (Millipore, USA) were electropho-

retically transferred after the reactions. A variety of primary antibodies were incubated overnight at 4°C on the membrane after blocking. By using enhanced chemiluminescence reagents (Zen-Bioscience, Chengdu, China), hybridization was detected after 1 hour at room temperature of incubation with different secondary antibodies. In order to quantify and analyze the specific bands on western blots, a BIO-RAD ChemiDocTM MP Imaging System was employed.

Cell viability assay

Cell viability was determined using the cell counting kit-8 (CCK-8; #K1018, APExBIO Technology LLC, USA). Briefly, cells (1×10^5/well/100 μL) were plated in 96-well plates and treated with ADM or Ara-C at various doses for the indicated times according to the manufacturer's instructions. The absorbance of each well was measured with a microplate reader after adding 10 μL of CCK-8 solution to each well and incubated at 37°C for another 2 h. For cell proliferation assay in vitro, cell suspension (5×10^3/well/100 μL) was inoculated in a 96-well plate. After incubating for 0, 1, 2, 3, and 4 days, each well was put in 10 μL of CCK8 and incubated for 2 h at 37°C.

EdU assay

EdU Cell Proliferation Kit (Meilunbio, Dalian, China) was adopted to inquire the cell proliferation ability. Cells were seeded at a cell density of 1×10^5/well in 12-well plates. Incubate with 20 μM EdU buffer for 1 hour at 37°C, fix with formaldehyde for 30 minutes, and permeabilize with 0.1% Triton X-100 for 15 minutes. After incubation, EdU solution was added and cell nucleus were stained with DAPI. The results were then observed under fluorescence microscope. Image j software was used to count EdU-positive cells.

Colony formation assay

Cells were seeded at a density of 1×10^3/well in 6-well plates and reconditioned to be filled with a 2-mL medium-agar mixture that consisted of two layers of 1.2 and 0.6% agar in the medium. The stock agar solution comprised 100 mL of distilled water and 6 g agar. After that, it was sterilized in an autoclave. After it became tepid, it was fractioned into two solutions using the medium. The bottom layer (1.2%) was left without cells, whereas the second layer contained cells cultured on 0.6% agar medium. While preparing each layer, it was necessary to solidify the plates for 10 or 15 min after pouring the agar solution into the wells. After the plates were incubated for two weeks, the colonies were photographed.

Measurements of S100P release

Serum from different groups of patients and normal healthy subjects were collected to measure S100P concentrations. Serum S100P release was measured using an enzyme-linked immunosorbent assay (ELISA) kit provided by Enzyme Biotechnology Co., Ltd. (Shanghai, China), evaluated according to the manufacturer's instructions.

Immunofluorescence analysis

The cells were immobilized in 4% formaldehyde at 20°C for half an hour before being permeabilized with 0.3% Triton X-100 at 4°C for 10 minutes. As soon as the samples had been saturated with goat serum for 1 h at room temperature, anti-LC3B antibody (#A19665, ABclonal), Alexa Fluor 488-conjugated immunoglobulin, and DAPI (Sigma) were used for immunofluorescence. Images were gathered with Leica TCS SP8 confocal microscope.

Electron microscopy

After collecting the cells, they were fixed in 2.5% glutaraldehyde for two hours. The samples were cut into 0.12-mm sections after embedding. A transmission electron microscope, H7500 (Hitachi, Tokyo, Japan), was used to examine the ultrathin sections.

Tumor cell xenograft model

From the Xiangya Medical College Animal Laboratory (Changsha, China), 16 specific pathogen-free-grade male BALB/c nude mice (aged 4 to 6 weeks) were purchased. The Animal Ethics Committee of Xiangya Medical College approval was obtained for all animal experiments. Four groups of mice were randomly divided in the experiment: (1) control shRNA grope taking PBS (vehicle); (2) control shRNA grope taking ADM; (3) S100P shRNA grope taking PBS (vehicle); and (4) S100P

shRNA grope taking ADM. Subcutaneous injections of control shRNA HL-60 cells and S100P shRNA HL-60 cells (1×10^7 cells/mouse) were administered to nude mice (weight, approximately 20 g) on the right flank. A tumor volume of 100 mm^3 was recorded at 0 days after 3-4 weeks. Then mice were intraperitoneally injected with ADM (2 mg/kg, every three days) for three weeks. The tumor volume (length × width × width × π/6) and body weight of the mice were monitored every three days. After treatment, mice were sacrificed, their tumors removed, imaged, weighted, and analyzed via IHC.

Immunohistochemistry

Tumors were fixed in 4% formaldehyde. Following dehydration and paraffin embedding, microtomes (Leica, Wetzlar, Germany) were used to slice specimens into 5-mm thick sections. The expressions of S100P, LC3B, p53, p-AMPK, and p-mTOR were examined via Immunohistochemistry. In order to unmask antigens, deparaffinized and rehydrated sections were pressure-cooked for 2 minutes in an antigen retrieval buffer (0.01 M citrate buffer, pH 6.0). After incubating with rabbit anti-S100P, LC3B, p53, p-AMPK and p-mTOR antibodies (1:200) overnight at 4°C, the sections were treated with biotinylated goat anti-rabbit IgG secondary antibodies for 1 hour at 37°C followed by streptavidin-HRP.

Statistical analysis

Statistical analysis included independently repeating each experiment at least three times and presenting the results as means and standard deviations. SPSS (version 19.0; IBM Corp., Armonk, NY, USA) and GraphPad Prism 7 (GraphPad Software Inc., San Diego, CA, USA) were used to analyze the quantitative results. Student's t-tests were used to compare two groups, and chi-square tests were used to compare S100P expression with clinicopathological features. $P<0.05$ was considered statistically significant.

Results

Correlation between S100P expression and clinical status in childhood AL

In this study, we used seven AL cell lines, namely MV4-11, THP-1, HL-60, KASUMI1, NALM-6, MOLT4, and Jurkat, to assess the expression of S100P via qRT-PCR and western blot analysis. Our results revealed varying levels of S100P expression in AL cells (**Figure 1A**, **1B**). The clinical relevance of S100P expression was further evaluated using qRT-PCR and enzyme-linked immunosorbent assay in BMMCs. Samples were collected from 45 patients diagnosed with ALL (23 in the primary phase, 6 in relapse, and 16 in CR), 26 patients with AML (16 in the primary phase, 4 in relapse, and 6 in CR), and eight healthy individuals serving as the control group. Higher levels of S100P expression were detected in individuals who achieved CR of leukemia and in healthy individuals (**Figure 1C**, **1D**), whereas lower levels were found in patients with primary and relapsed leukemia (**Figure 1C**, **1D**). These data suggest a correlation between S100P levels and the clinical status of childhood AL.

Subsequently, we investigated the potential association between S100P expression and clinical characteristics. Using the BMMC mRNA levels of 23 patients with ALL and 16 patients with AML, we employed the median value to categorize individuals into low- and high-expression groups. The results showed that the white blood cell count and risk classification were inversely correlated with S100P expression in patients with primary AL (**Tables 1**, **2**). Conversely, no significant relationship was observed between S100P expression and sex, age, platelet count, or hemoglobin levels (**Tables 1**, **2**). Thus, S100P reflects different clinical features of childhood AL.

S100P regulates leukemia cell proliferation and chemosensitivity

To investigate the potential role of S100P in regulating leukemic cell death, target shRNA against S100P or control shRNA were transfected into HL-60 and Jurkat cells (**Figures 2A**, **2B**, S1A, S1B). Our findings indicated that ADM and Ara-C induced growth inhibition in a dose-dependent manner in both control shRNA and vector groups (**Figures 2C**, S1C). Knockdown of S100P resulted in increased drug resistance in leukemia cells compared with that in the control (**Figure 2C**). In contrast, regulating S100P expression in leukemia cells made them significantly more sensitive to chemotherapeutic drugs than the vector group (Figure S1C). Additionally, the findings from cell proliferation, EdU, and suspended colony formation assays

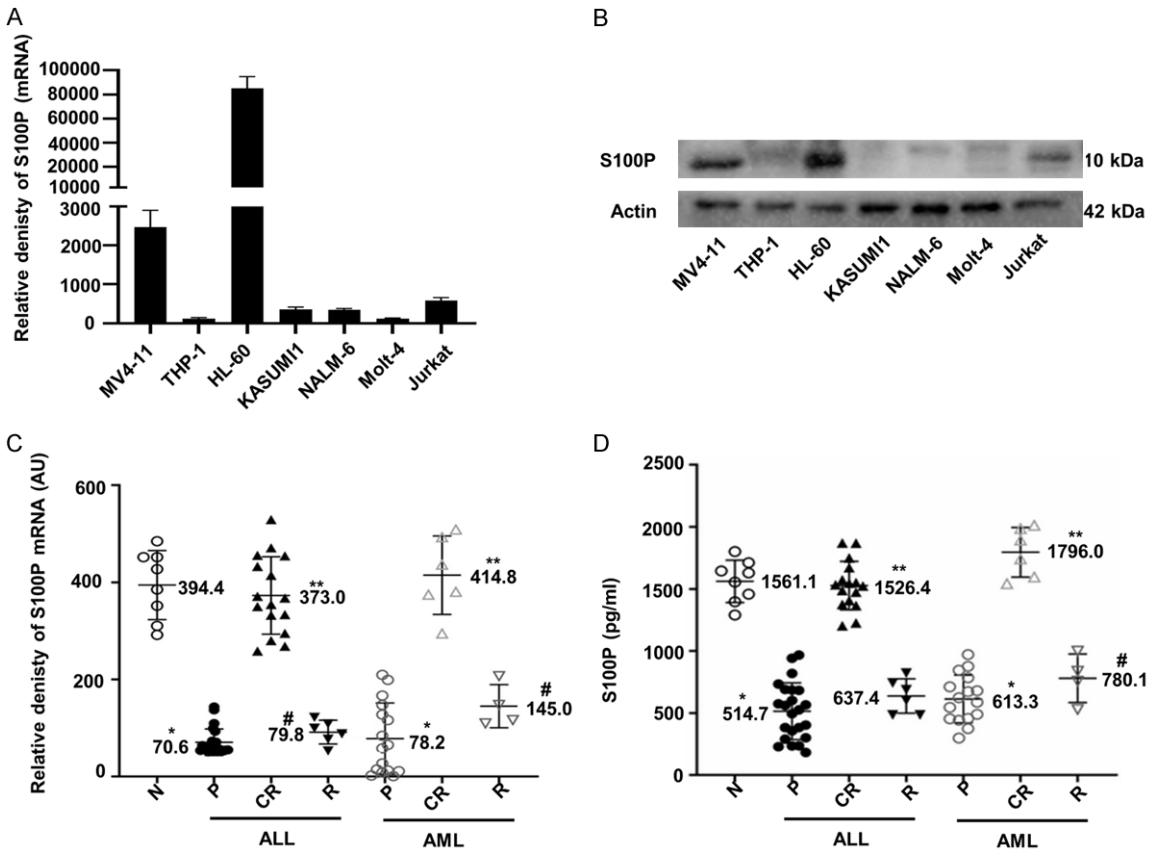

Figure 1. S100P was expressed in different cancer cell lines and correlated to the stage of childhood AL. A, B. QRT-PCR and western blot of S100P and actin in various cell lines hinted at an over-expression of S100P in HL-60 and Jurkat cell lines; C. Relative mRNA expression levels of S100P in childhood AL. ALL, acute lymphoblastic leukemia; AML, acute myeloid leukemia; N, normal healthy subject; P, primary; CR, complete remission; R, relapse. *P<0.05 vs. normal subject; **P>0.05 vs. normal subject; #P<0.05 vs. complete remission; D. Expression of S100P in serum of different patients and normal healthy subjects. The expression of S100P was significantly lower in primary and relapse patients than that in the complete remission patients. N, normal healthy subject; P, primary; CR, complete remission; R, relapse. *P<0.05 vs. normal subject; **P>0.05 vs. normal subject; #P<0.05 vs. complete remission.

demonstrated a significant increase in cell growth with S100P knockdown and a decrease in cell growth with S100P overexpression (**Figures 2D-F**, S1D-F). The expression levels of proliferation-related proteins, including cyclin D1, cyclin-dependent kinase 2, and B-cell lymphoma 2, were assessed in HL-60 and Jurkat cells. These proteins are upregulated in S100P-ablated cells and downregulated in S100P-overexpressing cells (**Figures 2G**, S1G). These results prove that S100P plays a crucial role in regulating the proliferation and chemosensitivity of leukemia cells.

S100P regulates autophagy in leukemia cells

The role of autophagy in chemotherapy resistance in hematological malignancies has become increasingly evident. To investigate the direct activation of autophagy by S100P and its regulation of the autophagic flux, the expression of microtubule-associated protein 1 light chain 3 (LC3) and SQSTM1/sequestosome 1 (p62) was determined using immunoblot analysis. LC3-II and p62 are widely used to monitor autophagy. A standard marker of autophagosomes, LC3-II, is generated by conjugating cytosolic LC3-I to phosphatidylethanolamine on nascent autophagosome surfaces [27]. The scaffold protein p62 serves as a substrate for autophagy, facilitating the transportation of ubiquitinated proteins for proteasomal degradation [27]. In the presence of S100P shRNA, classical autophagic stimuli in HBSS increased LC3-II expression and decreased p62 expression compared with the control group (**Figure**

Table 1. Association between S100P expression and clinicopathological characteristics in pediatric patients with ALL

Clinicopathologic features	Low expression (n=12) (%)	High expression(n=11) (%)	*p*-value[a]
Age at diagnosis (years)			P=0.32
<10	8 (66.7%)	10 (90.9%)	
≥10	4 (33.3%)	1 (9.1%)	
Gender			P=0.09
Male	5 (41.7%)	9 (81.8%)	
Female	7 (58.3%)	2 (18.2%)	
WBCs (× 10^9/l) at diagnosis	88.2 (15.6-576.9)[b]	17.4 (1.3-354.1)	P=0.04
Hb (g/l) at diagnosis	64 (3-97)	82 (43-133)	P=0.09
Plt (× 10^9/l) at diagnosis	65 (14-208)	69 (2-290)	P=0.25
Risk classification			P=0.04
Standard risk	1 (8.3%)	6 (54.5%)	
Medium risk	9 (75.0%)	5 (45.5%)	
High risk	2 (16.7%)	0 (0%)	

WBCs, white blood cells; Hb, hemoglobin; Plt, platelet; [a]*P*-value in Mann-Whitney U test and Chi-square test; [b]values shown as median minimum-maximum.

Table 2. Association between S100P expression and clinicopathological characteristics in pediatric patients with AML

Clinicopathologic features	Low expression (n=8) (%)	High expression (n=8) (%)	*p*-value[a]
Age at diagnosis (years)			P=1.00
<10	4 (50.0%)	4 (50.0%)	
≥10	4 (50.0%)	4 (50.0%)	
Gender			P=1.00
Male	6 (75.0%)	5 (62.5%)	
Female	2 (25.0%)	3 (37.5%)	
WBCs (× 10^9/l) at diagnosis	73.9 (1.7-244.3)[b]	11.8 (1.8-62.4)	P=0.03
Hb (g/l) at diagnosis	77 (42-111)	83 (74-109)	P=0.31
Plt (× 10^9/l) at diagnosis	45 (11-254)	50 (15-1360)	P=0.86
Risk classification			P=0.04
Standard risk	0 (0%)	0 (0%)	
Medium risk	2 (25.0%)	7 (87.5%)	
High risk	6 (75.0%)	1 (12.5%)	

WBCs, white blood cells; Hb, hemoglobin; PLT, platelet; [a]*P*-value in Mann-Whitney U test and Chi-square test; [b]values shown as median minimum-maximum.

3A, **3B**). Conversely, the overexpression of S100P through gene transfection led to a significant decrease in LC3-II expression and an increase in p62 levels (Figure S2A, S2B). Additionally, treatment with the lysosomal protease inhibitors pepstatin A and E64d (PA/E64d) increased LC3-II and p62 expression, regardless of the expression level of S100P (**Figures 3B**, S2B). This suggests that the increased LC3-II was not caused by decreased degradation of lipidated LC3 but rather by increased autophagic flux.

Traditionally, electron microscopy has been used to quantify autophagosomes. Type I autophagosomes are characterized by a double-membrane structure and contain undigested cytoplasmic contents that remain separate from lysosomes. Type II autophagolysosomes are hybrid organelles that combine autophagosomes and lysosomes, each with a single limiting membrane [27]. According to our electron microscopy analysis, S100P shRNA treatment resulted in higher numbers of autophagosomes and autophagolysosomes in leukemic cells

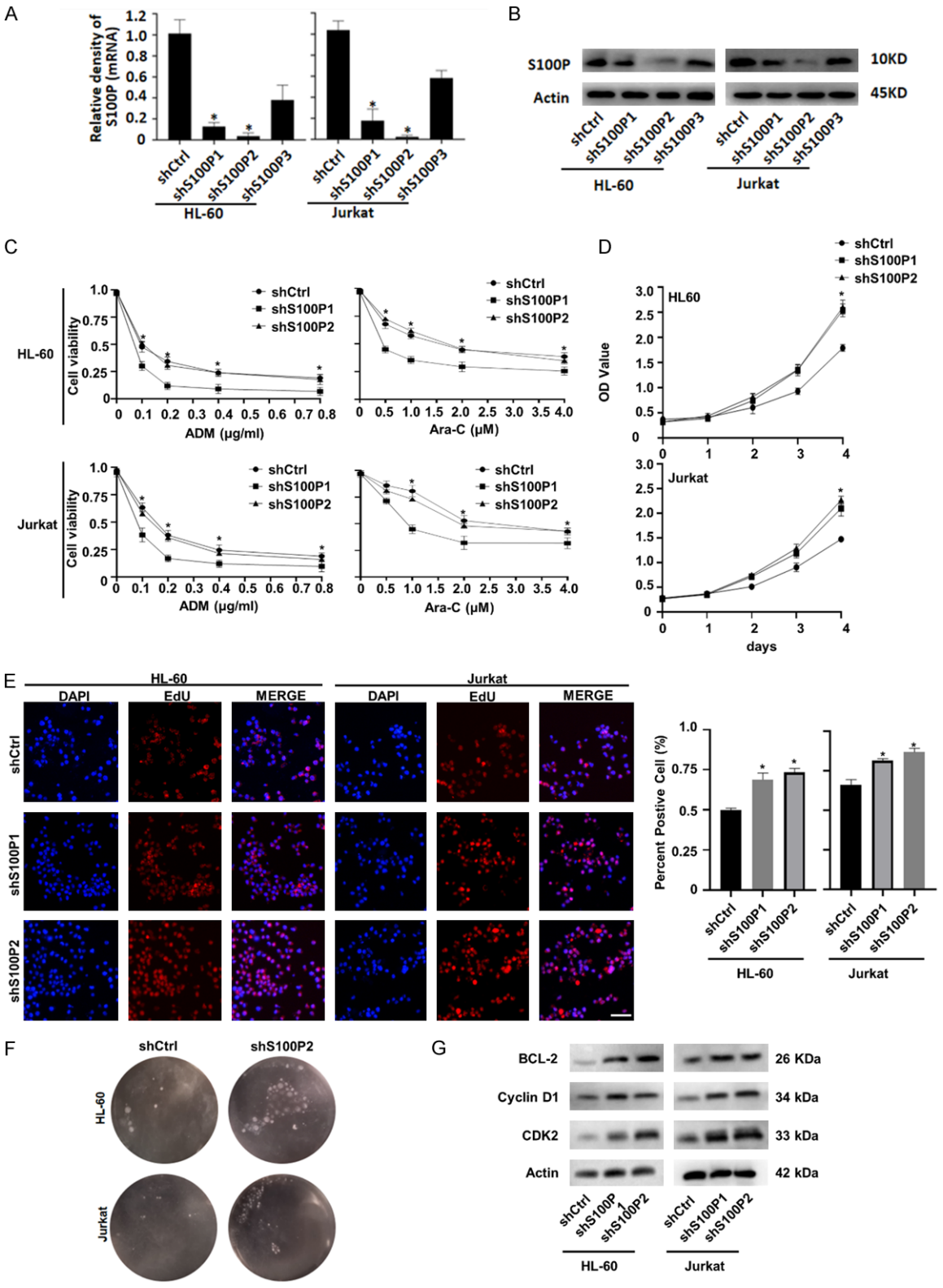

Figure 2. S100P knockdown increased leukemia cells proliferation and chemosensitivity. A, B. QRT-PCR and western blot analysis confirmed the downregulation of S100P in HL-60 and Jurkat cells treated with S100P shRNA. *P<0.05 vs. shCtrl group; C. S100P knockdown decreased the sensitivity of leukemia cells to anti-cancer drug. Knockdown S100P by shRNA in HL-60 and Jurkat cells and then treated with ADM and Ara-C at the indicated doses for 24 h and 48 h respectively. Cell viability was assayed using a CCK-8 kit (n=3, *P<0.05 vs. shCtrl group); D. S100P depletion increased the proliferation of HL-60 and Jurkat cells. HL-60 and Jurkat cells were transfected with S100P shRNA or

control shRNA and then cultured for 4 days. OD value was assayed using a CCK-8 kit for every day (n=3, *P<0.05 vs. shCtrl group); E. EdU assays were performed and analyzed. Representative EdU analysis of cell proliferation in HL-60 and Jurkat cells with S100P shRNA or control shRNA transfection. DAPI (blue) was used to stain nucleus and EdU (red) showed the incorporated cells. *P*-values have been calculated using paired Student's t-test. Scale bar: 50 μm (n=3, *P<0.05 vs. shCtrl group); F. S100P depletion enhanced the colony formation of HL-60 and Jurkat cells. HL-60 and Jurkat cells were transfected with S100P shRNA or control shRNA and then soft agarose colony formation were performed; G. S100P ablation contributed to increment of Cyclin D1, CDK2 and Bcl-2. HL-60 and Jurkat cells were transfected with S100P shRNA or control shRNA and then Cyclin D1, CDK2 and Bcl-2 levels were assayed by western blot.

than in control cells (**Figure 3C**). LC3 puncta showed a significant increase following S100P depletion, as observed using immunofluorescence (**Figure 3D**). In contrast, upregulated S100P expression was linked to decreased autophagosome, autophagolysosome, and LC3 puncta formation compared with the vector group (Figure S2C, S2D). These data demonstrate that leukemia cells exhibit typical autophagic reactions to HBSS and that endogenous S100P regulates autophagy initiation.

Autophagy is essential for endogenous S100P-regulated chemoresistance

Based on these findings, it is evident that S100P can regulate the proliferation of leukemia cells and autophagy. We investigated the relationship between autophagy and chemosensitivity using S100P. In this study, 3-methyladenine (3-MA), a PI3K inhibitor, was used to inhibit autophagy by inhibiting autophagy-dependent protein degradation and preventing autophagosome formation. Upon the reduction of S100P expression, the administration of 3-MA significantly suppressed the conversion of LC3 (LC3-I to LC3-II), formation of autophagosomes, and consumption of p62 was induced by HBSS (**Figure 4A**, **4B**). Additionally, 3-MA enhanced the effects of S100P overexpression on autophagy (Figure S3A, S3B). Furthermore, the application of chemotherapeutic drugs in conjunction with 3-MA treatment reversed the drug resistance induced by S100P in the S100P shRNA groups and further promoted the chemosensitivity of leukemia cells by introducing the S100P vector (**Figures 4C**, **4D**, S3C, S3D). These findings suggested that endogenous S100P-mediated chemoresistance in leukemic cells requires autophagy.

p53/AMPK/mTOR pathway is required for S100P-mediated autophagy regulating chemosensitivity

The transcription factor p53, a tumor suppressor, is responsive to various cellular stressors, such as DNA damage, oncogenesis, oxidative stress, and hypoxia [28]. Furthermore, p53 plays a crucial role in the regulation of autophagy, as evidenced by studies indicating that its subcellular localization influences this process [29]. Nuclear p53 promotes autophagy by transactivating the target genes, whereas cytoplasmic p53 predominantly inhibits autophagy [30, 31]. Our results showed that endogenous S100P could regulate autophagy in leukemia cells; however, it remains unclear whether S100P affects autophagy by controlling the cytonuclear trafficking of p53. Our study showed that S100P overexpression increased p53 expression, whereas S100P knockdown suppressed p53 expression (**Figure 5A**). Moreover, we observed that the depletion of S100P in leukemia cells hindered the translocation of p53 from the nucleus to the cytosol (**Figures 5B**, S4). In contrast, the upregulation of S100P expression boosted p53 translocation (**Figures 5B**, S4). To further investigate whether S100P knockdown promoted autophagy by p53, we activated p53 with Tenovin-6, a pharmacological p53 activator. Compared with leukemia cells with S100P depletion, adding Tenovin-6 to S100P-deficient cells significantly decreased LC3-II and increased p62 expression levels (**Figure 5C**). These findings indicate that p53 mediates S100P-regulated autophagy in leukemia cells.

To investigate the potential regulatory role of S100P in the p53/AMPK/mTOR pathway in leukemia cells, we subjected these cells to nutrient deprivation by treating them with HBSS, with or without various activators or inhibitors of the pathway [32]. Suppression of S100P expression resulted in a notable reduction in the levels of p53 and phosphorylated mTOR (p-mTOR) while concurrently increasing the phosphorylated AMPK (p-AMPK) level compared with the control group (**Figure 5C**, **5D**). Administration of Tenovin-6 (a p53 activator) effectively reversed the alterations in p53,

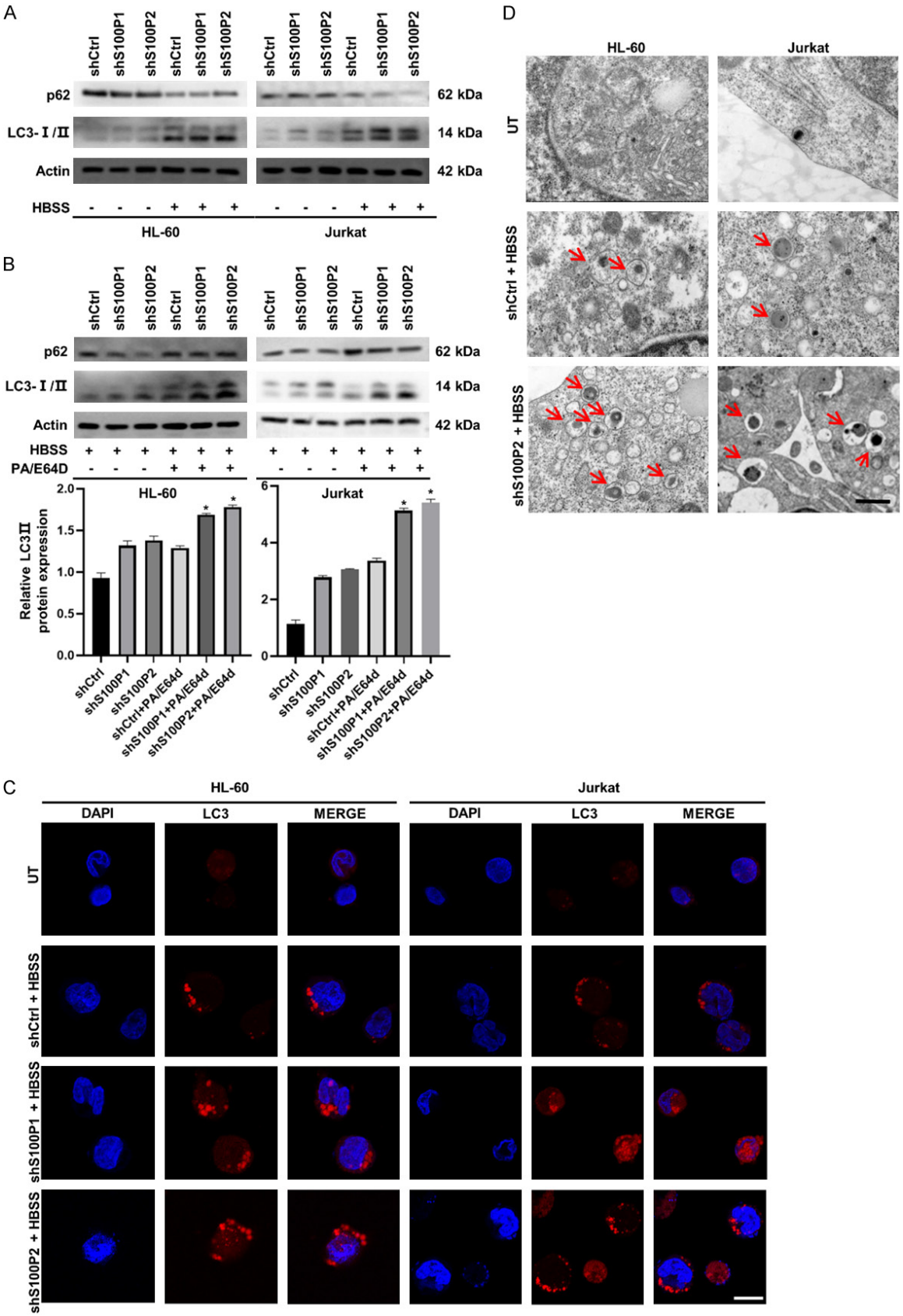

Figure 3. S100P knockdown increased HBSS-induced autophagy in leukemia cells. A. HL-60 and Jurkat cells were transfected with S100P shRNA or control shRNA and then starved by HBSS for 2 h. LC3-I/II and p62 levels were as-

sayed by western blot; B. HL-60 and Jurkat cells were transfected with S100P shRNA or control shRNA and then pre-treated for 1 h with pepstatin A (PA, 10 μM) and E64d (10 μM) as indicated. Cells were subsequently treated for 2 h with HBSS in continuous presence or absence PA/E64d inhibitors. LC3-I/II and p62 levels were assayed by western blot (n=3, *P<0.05 vs. shS100P group); C. Ultrastructural features in HL-60 and Jurkat cells transfected with S100P shRNA or control shRNA after 2 h treatment of HBSS. More autophagolysosomes were seen in S100P shRNA plus HBSS-treated cells than in cells treated with control shRNA plus HBSS. Red arrows indicated autophagolysosomes. Scale bar: 500 nm; D. HL-60 and Jurkat cells were transfected with S100P shRNA or control shRNA and then starved by HBSS for 2 h and then immunostained with LC3B-specifc antibody (red) and DAPI (blue). Scale bar: 10 μm.

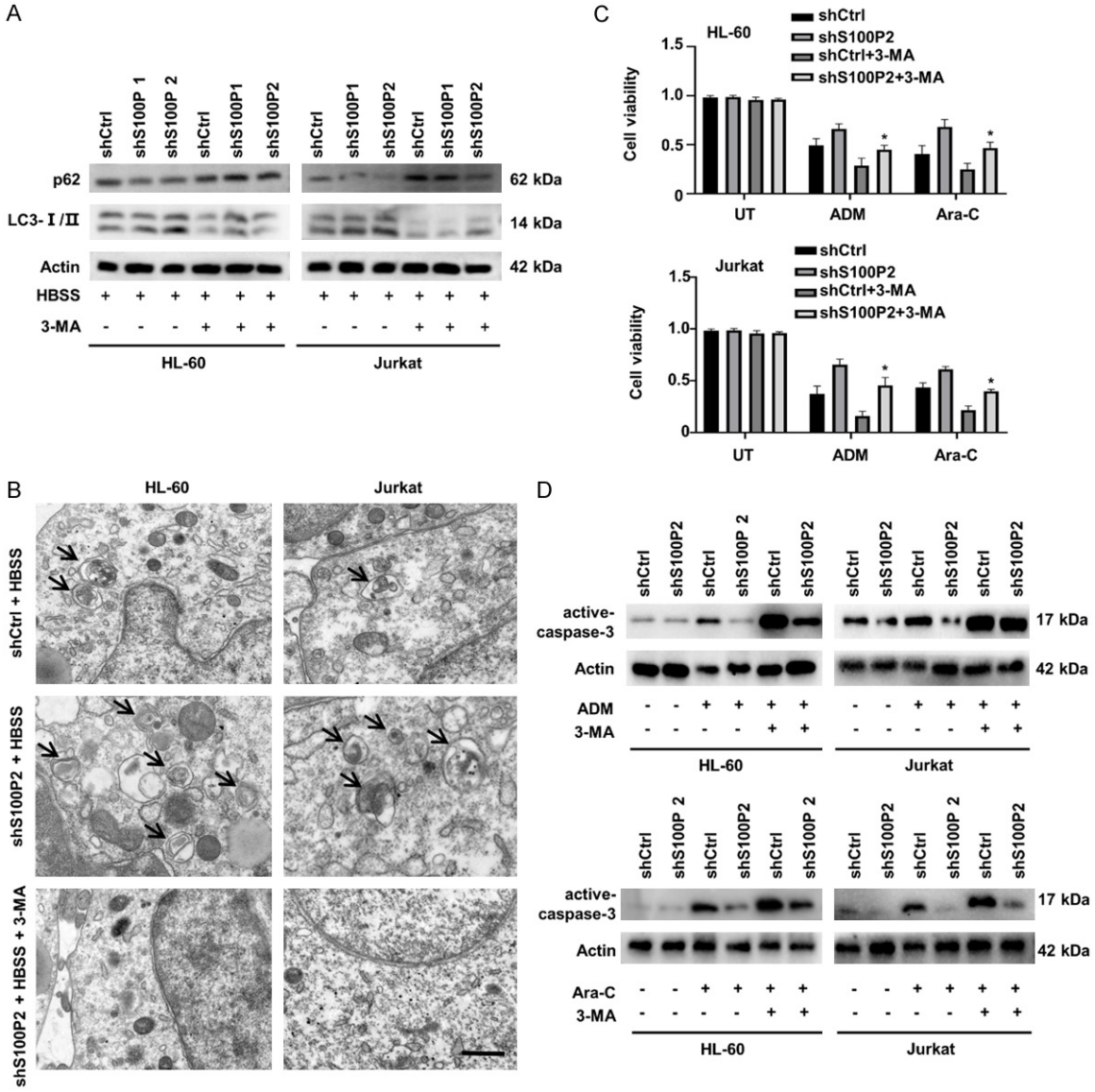

Figure 4. Inhibition of autophagy reversed S100P knockdown-mediated drug resistance. A, B. Inhibitor of autophagy blocked the initiation of autophagy. Analysis of LC3 and p62 expressions by western blot and number of autophagosomes by electron microscopy in the presence or absence of 3-MA (10 mM) treatment for 1 h in S100P shRNA or control shRNA cells, followed by treatment with HBSS for 2 h. Black arrows indicate autophagosomes. Scale bar: 500 nm; C. Inhibition of autophagy reversed S100P knockdown-mediated drug resistance. HL-60 and Jurkat cells were transfected with S100P shRNA or control shRNA and then pre-treated for 1 h with 3-MA (10 mM) as indicated. Cells were subsequently treated for 24 h with ADM (0.2 μg/ml) or 48 h with Ara-C (4 μM), then cell viability was assayed using a CCK-8 kit (n=3, *P<0.05 vs. shS100P group); D. Inhibition of autophagy reversed S100P knockdown-mediated cells survive. HL-60 and Jurkat cells were transfected with S100P shRNA or control shRNA and then pre-treated for 1 h with 3-MA (10 mM) as indicated. Cells were subsequently treated for 24 h with ADM (0.2 μg/ml), then active caspase-3 levels were assayed by western blot.

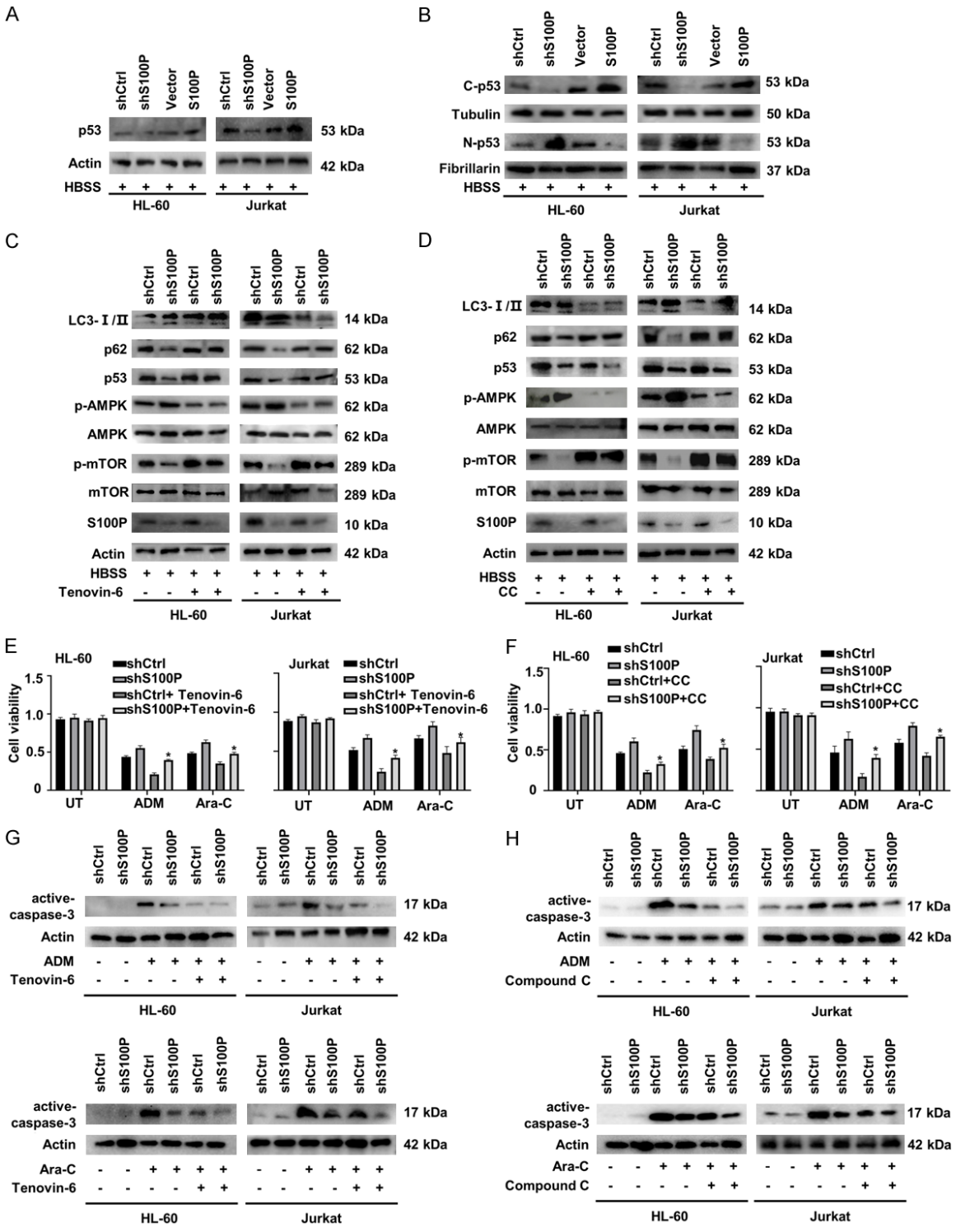

Figure 5. p53/AMPK/mTOR pathway was required for S100P-mediated autophagy regulating chemosensitivity. A. p53 expression levels were detected in S100P-deficient cells and S100P-overexpression cells by western blot analysis respectively; B. The expressions of nuclear/cytosolic p53 in S100P-deficient cells and S100P-overexpression cells were assayed by western blot. Fibrillarin was a nuclear fraction control and tubulin was a cytoplasmic fraction control. C-p53, cytosolic p53; N-p53, nuclear p53; C. HL-60 and Jurkat cells were transfected with S100P shRNA or control shRNA and then pre-treated with Tenovin-6 (5 μM) for 8 h. Cells were subsequently treated for 2 h with HBSS, and then LC3-I/II, p62, p53, p-AMPK, AMPK, p-mTOR, mTOR, and S100P levels were assayed by western blot (n=3, *P<0.05 vs. shS100P group, #P>0.05 vs. shS100P group); D. HL-60 and Jurkat cells were transfected with

S100P shRNA or control shRNA and then pre-treated with Compound C (20 μM) for 6 h. Cells were subsequently treated for 2 h with HBSS, and then LC3-I/II, p62, p53, p-AMPK, AMPK, p-mTOR and mTOR levels were assayed by western blot. CC, Compound C (n=3, *P<0.05 vs. shS100P group, #P>0.05 vs. shS100P group); E. HL-60 and Jurkat cells were transfected with S100P shRNA or control shRNA and then pre-treated with Tenovin-6 (5 μM) for 8 h. Cells were subsequently treated for 24 h with ADM (0.2 μg/ml) or 48 h with Ara-C (4 μM), then cell viability was assayed using a CCK-8 kit (n=3, *P<0.05 vs. shS100P group); F. HL-60 and Jurkat cells were transfected with S100P shRNA or control shRNA and then pre-treated with Compound C (20 μM) for 6 h. Cells were subsequently treated for 24 h with ADM (0.2 μg/ml) or 48 h Ara-C (4 μM), then cell viability was assayed using a CCK-8 kit. CC, Compound C (n=3, *P<0.05 vs. shS100P group); G. HL-60 and Jurkat cells were transfected with S100P shRNA or control shRNA and then pre-treated with Tenovin-6 (5 μM) for 8 h. Cells were subsequently treated for 24 h with ADM (0.2 μg/ml), then active caspase-3 levels were assayed by western blot; H. HL-60 and Jurkat cells were transfected with S100P shRNA or control shRNA and then pre-treated with Compound C (20 μM) for 6 h. Cells were subsequently treated for 24 h with ADM (0.2 μg/ml), and then active caspase-3 levels were assayed by western blot.

p-AMPK, and p-mTOR expression induced by S100P knockdown, indicating that p53 acts as a downstream signaling molecule of S100P (**Figure 5C**). Compound C, an AMPK inhibitor, inhibited the expression of p-AMPK and promoted the expression of p-mTOR. There was no significant effect on p53 levels, suggesting that AMPK is downstream of the S100P/p53 pathway (**Figure 5D**). Furthermore, compared with leukemia cells with S100P depletion, the addition of Compound C to S100P-deficient cells also significantly decreased LC3-II and increased p62 expression levels (**Figure 5D**), suggesting that S100P mediates autophagy through the p53/AMPK/mTOR pathway.

To ascertain the significance of p53 and AMPK in the chemosensitivity of leukemia cells mediated by S100P, the viability of cells treated with chemotherapeutic drugs was assessed in the presence or absence of Tenovin-6 or Compound C. The reduction of S100P expression through knockdown decreased the chemosensitivity of leukemia cells treated with ADM and Ara-C, as treated leukemia cells compared with the control group (**Figure 5E**, **5F**). Furthermore, the assessment of active caspase-3 levels provided evidence that administering chemotherapeutic drugs, preceded by Tenovin-6 or Compound C pretreatment, partially mitigated the reversed S100P-induced drug resistance in the S100P shRNA groups (**Figure 5G**, **5H**). This finding suggests that the p53/AMPK/mTOR pathway plays a crucial role in the S100P regulation of chemosensitivity in leukemia cells influenced by S100P.

Knockdown of S100P expression inhibits the anticancer activity of ADM in vivo

The aforementioned studies demonstrate that S100P-mediated autophagy plays a role in regulating chemosensitivity in AL cells in vitro. To assess the impact of S100P in vivo, we subcutaneously injected S100P shRNA and control shRNA HL-60 cells (1×10^7 cells/mouse) into nude mice and subsequently conducted animal experiments. In the treatment group, an intraperitoneal injection of ADM (2 mg/kg every three days) was given when subcutaneous tumors were measurable at 100 mm^3 for the subsequent three weeks. A significant reduction in tumor size and weight was observed in the control shRNA model treated with ADM compared with the S100P shRNA model treated with ADM (**Figure 6A-C**). Similar to the findings of the in vitro experiments, the knockdown of S100P expression enhanced the expression of LC3B and p-AMPK and decreased the expression of p53 and phosphorylated mTOR (p-mTOR) in nude mice (**Figure 6D**), indicating an antitumor effect via S100P-mediated autophagy through the p53/AMPK/mTOR pathway.

Discussion

There is a growing body of evidence suggesting a potential correlation between S100 proteins and disease progression and prognosis various tumor types, such as breast, head, neck, lung, colorectal, melanoma, and hematological malignancies, may be associated with S100 proteins [19, 33-36]. Several proteins associated with AML, namely S100A4, S100A6, S100A8, S100A9, S100A10, and S100P, have been reported to play crucial roles [37, 38]. Our previous study showed that S100A8-driven autophagy promotes chemoresistance in leukemia cells [38]; however, endogenous S100P expression and its function in mediating autophagy and regulating chemoresistance in leukemia remain unclear. This study demon-

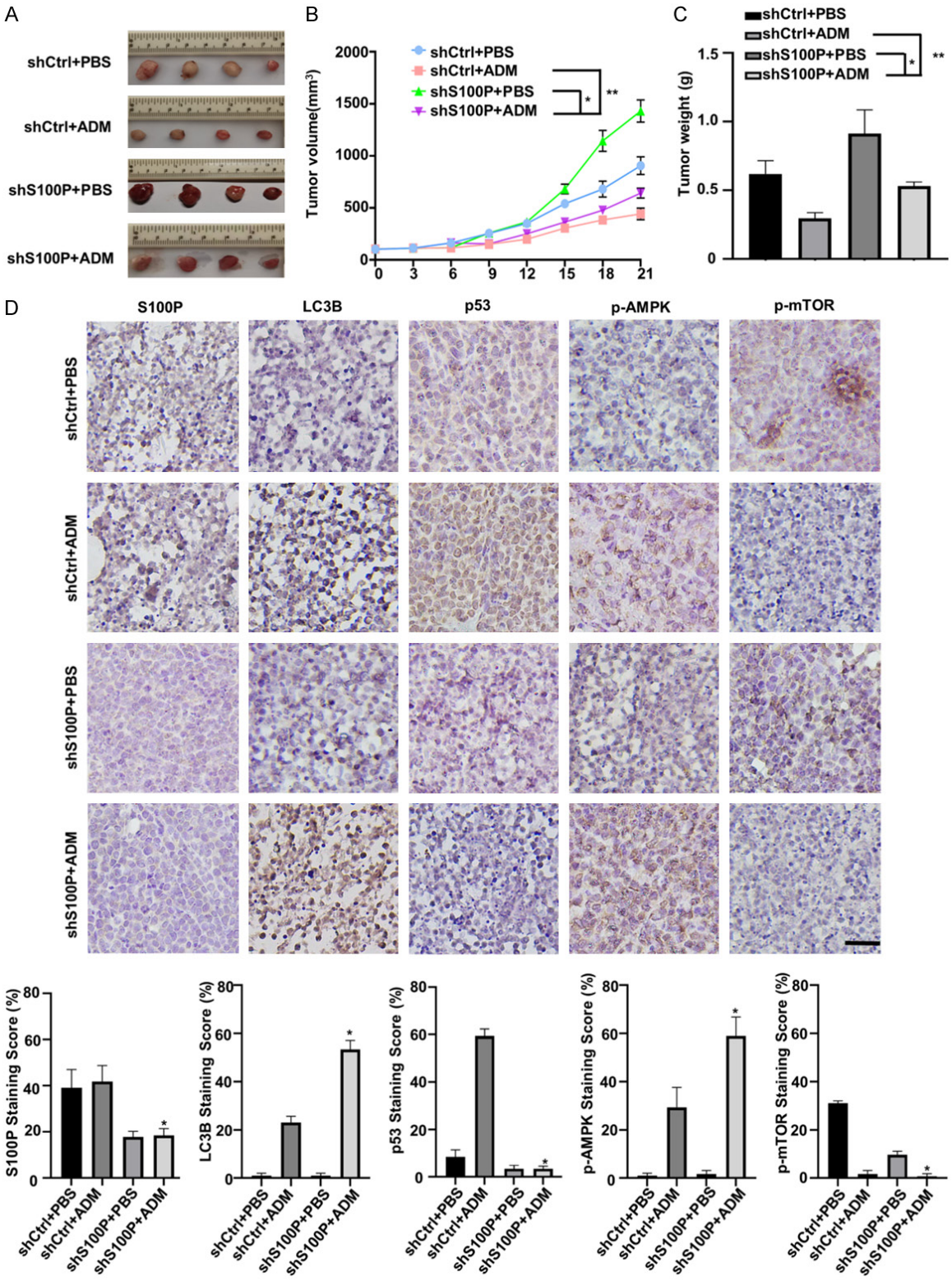

Figure 6. Knockdown of S100P expression inhibited anticancer activity of ADM in vivo. A-C. BALB/c nude mice were injected subcutaneously with S100P shRNA HL-60 cells (1×10^7 cells/mouse). After 3-4 weeks, adriamycin (ADM 2 mg/kg, every three days) were intraperitoneally injected into the mice for 3 weeks. Tumor volumes were measured every three days. At the termination of the experiments, all xenografts were removed, imaged and weighted (n=4 mice/group, *P<0.05, **P<0.05, #P>0.05); D. Immunohistochemical staining of S100P, LC3B, p53, p-AMPK and p-mTOR were performed with an isolated tumor at the termination of the experiments. All experiments were conducted in triplicate. Scale bar: 100 μm (n=3, *P<0.05 vs. shS100P group).

strated the abundant expression of S100P in a diverse range of blood and non-blood cancer cell lines. Moreover, a negative correlation was observed between S100P expression and clinical status in childhood leukemia. These findings suggest that S100P negatively regulates autophagy and chemosensitivity in leukemia cells, potentially via the p53/AMPK/mTOR-dependent pathway. These results have significant implications for developing novel therapeutic approaches for patients with AL.

Chemoresistance, a multifaceted phenomenon affecting the efficacy of chemotherapeutic agents, is responsible for the mortality of over 90% of cancer patients. Successful treatment of leukemia is progressively challenging owing to the emergence of drug resistance. Substantial evidence suggests that S100P is closely linked to chemoresistance in various carcinomas, such as those affecting the pancreas, prostate, stomach, and breast [39-42]. This study showed that elevated S100P expression in leukemia cells resulted in increased susceptibility to ADM and Ara-C while impeding cell proliferation. In contrast, suppression of S100P expression decreased the sensitivity of leukemia cells to these chemotherapeutic agents and facilitated cell proliferation. Consequently, S100P exerts a substantial influence on the chemoresistance of leukemia cells. The available data indicate that autophagy can serve as a protective mechanism that confers resistance to chemotherapy, induces autophagic cell death, and enhances sensitivity to chemotherapy [43, 44]. We previously found that autophagy plays a crucial role in leukemic pathogenesis and chemotherapeutic resistance [11, 15, 21, 45]; however, little is known about its association with endogenous S100P. In this study, we demonstrated a significant reduction in HBSS-induced autophagy as a result of S100P upregulation. However, through targeted modulation of S100P, we successfully enhanced starvation-induced autophagy and effectively suppressed it using the autophagy inhibitor 3-MA. Consequently, this intervention increased the susceptibility of leukemia cells to chemotherapy. Moreover, our observations highlight a robust correlation between autophagy and chemoresistance in leukemia cells, underscoring the pivotal role of endogenous S100P.

Furthermore, we hypothesized that the pro-autophagic effects of S100P are mediated through the p53/AMPK/mTOR pathway. Cancer prevention and suppression depend on p53, a transcription activator [46]. It has been shown that p53 plays a dual role in autophagy regulation. Upon exposure to genotoxic stress or starvation, p53 is activated, which induces autophagy [47, 48]. Conversely, inactivating p53 through deletion, depletion, or inhibition by pifithrin-α can trigger autophagy. p53 regulates autophagy depending on its subcellular localization [29]. Autophagy is facilitated by nuclear p53 through the transactivation of its target genes, whereas it is primarily suppressed by cytoplasmic p53 [30, 31]. In this study, we observed that the depletion of S100P considerably enhanced starvation-induced autophagy and reduced p53 and cytoplasmic p53 levels. Moreover, the administration of Tenovin-6, a p53 activator, impeded the regulation of starvation-induced autophagy mediated by S100P. These findings suggest that S100P induces autophagy in leukemic cells in the presence of p53.

Additionally, we propose that the AMPK/mTOR pathway functions as a downstream signal for p53 to regulate autophagy via S100P. The AMPK/mTOR signaling pathway is a pivotal regulator of cellular autophagy [13, 49]. By sensing energy molecules, AMPK regulates autophagy by downregulating mTOR phosphorylation to adjust energy metabolism [50]. Our results suggested that the knockdown of S100P significantly increased AMPK phosphorylation and decreased mTOR phosphorylation. Moreover, treatment with Tenovin-6 inhibited S100P-based regulation of HBSS-induced AMPK phosphorylation, suggesting that AMPK is a downstream gene of p53. In addition, pharmacological inhibition of AMPK (Compound C) also inhibited the regulation by S100P of HBSS-induced phosphorylation of mTOR and autophagy, suggesting that AMPK/mTOR is required for S100P-mediated autophagy in leukemia cell chemoresistance. Furthermore, notable enhancements in the dimensions of HL-60 xenografts and LC3B and AMPK expression levels were observed in nude mice upon the inhibition of S100P. Consequently, the presented evidence suggests that S100P-mediated autophagy may be a therapeutic target for leukemia.

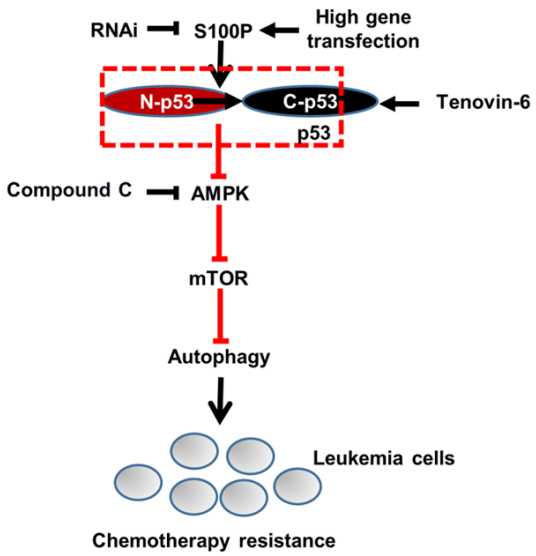

Figure 7. Schematic of the mechanism by which S100P modulates drug resistance by regulating autophagy. Endogenous S100P was overexpressed in blood cancer cell lines and functions as a negative regulator of autophagy, which inhibited resistance to anticancer therapies through p53/AMPK/mTOR pathway. Pharmacological inhibition (for example, Tenovin-6 and Compound C) of the p53/AMPK/mTOR pathway reverses the resistance of S100P ablation's leukemia cells to chemotherapy.

Endogenous S100P is expressed in blood cancer cell lines and functions as a negative regulator of autophagy, thereby inhibiting resistance to anticancer therapies. As an S100 calcium-binding protein, S100P regulates p53 expression and cytoplasmic translocation and affects the AMPK/mTOR pathway, thereby regulating leukemia cell autophagy and chemosensitivity (**Figure 7**). The findings presented in this study provide further evidence for the role of endogenous S100P in autophagy and chemoresistance in leukemic cells, which may enable more effective leukemia chemotherapy by affecting autophagy and modifying leukemic chemoresistance.

Acknowledgements

We would like to thank Editage (www.editage.cn) for English language editing. This work was supported by the National Natural Science Foundation of China (No. 81770178 and No. 82000137), and the Natural Science Foundation of Hunan Province of China (No. 2020JJ4918 and No. 2021JJ40318).

Written informed consent was obtained from each subject involved.

Disclosure of conflict of interest

None.

Address correspondence to: Dr. Liangchun Yang, Department of Pediatrics, Xiangya Hospital Central South University, No. 87, Xiangya Road, Changsha 410008, Hunan, The People's Republic of China. E-mail: 405010@csu.edu.cn

References

[1] Hunger SP and Mullighan CG. Acute lymphoblastic leukemia in children. N Engl J Med 2015; 373: 1541-1552.
[2] Malard F and Mohty M. Acute lymphoblastic leukaemia. Lancet 2020; 395: 1146-1162.
[3] Lamble AJ and Tasian SK. Opportunities for immunotherapy in childhood acute myeloid leukemia. Blood Adv 2019; 3: 3750-3758.
[4] Zhao H, Wei J, Wei G, Luo Y, Shi J, Cui Q, Zhao M, Liang A, Zhang Q, Yang J, Li X, Chen J, Song X, Jing H, Li Y, Hao S, Wu W, Tan Y, Yu J, Zhao Y, Lai X, Yin ETS, Wei Y, Li P, Huang J, Wang T, Blaise D, Xiao L, Chang AH, Nagler A, Mohty M, Huang H and Hu Y. Pre-transplant MRD negativity predicts favorable outcomes of CAR-T therapy followed by haploidentical HSCT for relapsed/refractory acute lymphoblastic leukemia: a multi-center retrospective study. J Hematol Oncol 2020; 13: 42.
[5] Ramos P and Bentires-Alj M. Mechanism-based cancer therapy: resistance to therapy, therapy for resistance. Oncogene 2015; 34: 3617-3626.
[6] Bosc C, Selak MA and Sarry JE. Resistance is futile: targeting mitochondrial energetics and metabolism to overcome drug resistance in cancer treatment. Cell Metab 2017; 26: 705-707.
[7] Spirina LV, Avgustinovich AV, Afanas'ev SG, Cheremisina OV, Volkov MY, Choynzonov EL, Gorbunov AK and Usynin EA. Molecular mechanism of resistance to chemotherapy in gastric cancers, the role of autophagy. Curr Drug Targets 2020; 21: 713-721.
[8] Yang Y and Klionsky DJ. Autophagy and disease: unanswered questions. Cell Death Differ 2020; 27: 858-871.
[9] Mulcahy Levy JM and Thorburn A. Autophagy in cancer: moving from understanding mechanism to improving therapy responses in patients. Cell Death Differ 2020; 27: 843-857.
[10] Duan R, Xie H and Liu ZZ. The role of autophagy in osteoarthritis. Front Cell Dev Biol 2020; 8: 608388.

[11] Liu L, Yang M, Kang R, Wang Z, Zhao Y, Yu Y, Xie M, Yin X, Livesey KM, Lotze MT, Tang D and Cao L. HMGB1-induced autophagy promotes chemotherapy resistance in leukemia cells. Leukemia 2011; 25: 23-31.
[12] Li X, He S and Ma B. Autophagy and autophagy-related proteins in cancer. Mol Cancer 2020; 19: 12.
[13] Saikia R and Joseph J. AMPK: a key regulator of energy stress and calcium-induced autophagy. J Mol Med (Berl) 2021; 99: 1539-1551.
[14] Kim J, Kundu M, Viollet B and Guan KL. AMPK and mTOR regulate autophagy through direct phosphorylation of Ulk1. Nat Cell Biol 2011; 13: 132-141.
[15] Yang L, Yu Y, Kang R, Yang M, Xie M, Wang Z, Tang D, Zhao M, Liu L, Zhang H and Cao L. Upregulated autophagy by endogenous high mobility group box-1 promotes chemoresistance in leukemia cells. Leuk Lymphoma 2012; 53: 315-322.
[16] Zhang H, Wang G, Ding Y, Wang Z, Barraclough R, Rudland PS, Fernig DG and Rao Z. The crystal structure at 2Å resolution of the Ca^{2+}-binding protein S100P. J Mol Biol 2003; 325: 785-794.
[17] Camara R, Ogbeni D, Gerstmann L, Ostovar M, Hurer E, Scott M, Mahmoud NG, Radon T, Crnogorac-Jurcevic T, Patel P, Mackenzie LS, Chau DYS, Kirton SB and Rossiter S. Discovery of novel small molecule inhibitors of S100P with in vitro anti-metastatic effects on pancreatic cancer cells. Eur J Med Chem 2020; 203: 112621.
[18] Kikuchi K, McNamara KM, Miki Y, Iwabuchi E, Kanai A, Miyashita M, Ishida T and Sasano H. S100P and ezrin promote trans-endothelial migration of triple negative breast cancer cells. Cell Oncol (Dordr) 2019; 42: 67-80.
[19] Prica F, Radon T, Cheng Y and Crnogorac-Jurcevic T. The life and works of S100P - from conception to cancer. Am J Cancer Res 2016; 6: 562-576.
[20] Arumugam T and Logsdon CD. S100P: a novel therapeutic target for cancer. Amino Acids 2011; 41: 893-899.
[21] Yang L, Yang M, Zhang H, Wang Z, Yu Y, Xie M, Zhao M, Liu L and Cao L. S100A8-targeting siRNA enhances arsenic trioxide-induced myeloid leukemia cell death by down-regulating autophagy. Int J Mol Med 2012; 29: 65-72.
[22] Yao J, Wang J, Xu Y, Guo Q, Sun Y, Liu J, Li S, Guo Y and Wei L. CDK9 inhibition blocks the initiation of PINK1-PRKN-mediated mitophagy by regulating the SIRT1-FOXO3-BNIP3 axis and enhances the therapeutic effects involving mitochondrial dysfunction in hepatocellular carcinoma. Autophagy 2022; 18: 1879-1897.
[23] Zhang H, Wan Y, Wang H, Cai J, Yu J, Hu S, Fang Y, Gao J, Jiang H, Yang M, Liang C, Jin R, Tian X, Ju X, Hu Q, Jiang H, Li Z, Wang N, Sun L, Leung AWK, Wu X, Qian X, Qian M, Li Ck, Yang J, Tang J, Zhu X, Shen S, Zhang L, Pui CH and Zhai X. Prognostic factors of childhood acute lymphoblastic leukemia with TCF3::PBX1 in CCCG-ALL-2015: a multicenter study. Cancer 2023; 129: 1691-1703.
[24] Yang W, Cai J, Shen S, Gao J, Yu J, Hu S, Jiang H, Fang Y, Liang C, Ju X, Wu X, Zhai X, Tian X, Wang N, Liu A, Jiang H, Jin R, Sun L, Yang M, Leung AWK, Pan K, Zhang Y, Chen J, Zhu Y, Zhang H, Li C, Yang JJ, Cheng C, Li CK, Tang J, Zhu X and Pui CH. Pulse therapy with vincristine and dexamethasone for childhood acute lymphoblastic leukaemia (CCCG-ALL-2015): an open-label, multicentre, randomised, phase 3, non-inferiority trial. Lancet Oncol 2021; 22: 1322-1332.
[25] Wang P, Xiong H, Li JX, Wang Z, Yang L, Tao F, Chen Z, Du Y, Zhang AP and Luo LL. Clinical analysis of pediatric acute myeloid leukemia with CCLG-AML 2015 regimen. Zhongguo Shi Yan Xue Ye Xue Za Zhi 2022; 30: 373-380.
[26] Livak KJ and Schmittgen TD. Analysis of relative gene expression data using real-time quantitative PCR and the 2-ΔΔCT method. Methods 2001; 25: 402-408.
[27] Mizushima N, Yoshimori T and Levine B. Methods in mammalian autophagy research. Cell 2010; 140: 313-326.
[28] Fischer M. Census and evaluation of p53 target genes. Oncogene 2017; 36: 3943-3956.
[29] Tasdemir E, Chiara Maiuri M, Morselli E, Criollo A, D'Amelio M, Djavaheri-Mergny M, Cecconi F, Tavernarakis N and Kroemer G. A dual role of p53 in the control of autophagy. Autophagy 2008; 4: 810-814.
[30] Tang J, Di J, Cao H, Bai J and Zheng J. p53-mediated autophagic regulation: a prospective strategy for cancer therapy. Cancer Lett 2015; 363: 101-107.
[31] Tasdemir E, Maiuri MC, Galluzzi L, Vitale I, Djavaheri-Mergny M, D'Amelio M, Criollo A, Morselli E, Zhu C, Harper F, Nannmark U, Samara C, Pinton P, Vicencio JM, Carnuccio R, Moll UM, Madeo F, Paterlini-Brechot P, Rizzuto R, Szabadkai G, Pierron G, Blomgren K, Tavernarakis N, Codogno P, Cecconi F and Kroemer G. Regulation of autophagy by cytoplasmic p53. Nat Cell Biol 2008; 10: 676-687.
[32] Feng Z, Hu W, de Stanchina E, Teresky AK, Jin S, Lowe S and Levine AJ. The regulation of AMPK β1, TSC2, and PTEN expression by p53: stress, cell and tissue specificity, and the role of these gene products in modulating the IGF-1-AKT-mTOR pathways. Cancer Res 2007; 67: 3043-3053.
[33] Laouedj M, Tardif MR, Gil L, Raquil MA, Lachhab A, Pelletier M, Tessier PA and Barabé F.

S100A9 induces differentiation of acute myeloid leukemia cells through TLR4. Blood 2017; 129: 1980-1990.
[34] Prieto D, Sotelo N, Seija N, Sernbo S, Abreu C, Durán R, Gil M, Sicco E, Irigoin V, Oliver C, Landoni AI, Gabus R, Dighiero G and Oppezzo P. S100-A9 protein in exosomes from chronic lymphocytic leukemia cells promotes NF-κB activity during disease progression. Blood 2017; 130: 777-788.
[35] Parkkila S, Pan PW, Ward A, Gibadulinova A, Oveckova I, Pastorekova S, Pastorek J, Martinez AR, Helin HO and Isola J. The calcium-binding protein S100P in normal and malignant human tissues. BMC Clin Pathol 2008; 8: 2.
[36] Yang XY, Jin J, Huang J, Li P, Xue JW, Wu XJ and He ZX. Expression and clinical significance profile analysis of S100 family members in human acute myeloid leukemia. Eur Rev Med Pharmacol Sci 2020; 24: 7324-7334.
[37] Brenner AK and Bruserud Ø. S100 proteins in acute myeloid leukemia. Neoplasia 2018; 20: 1175-1186.
[38] Mondet J, Chevalier S and Mossuz P. Pathogenic roles of S100A8 and S100A9 proteins in acute myeloid and lymphoid leukemia: clinical and therapeutic impacts. Molecules 2021; 26: 1323.
[39] Dakhel S, Padilla L, Adan J, Masa M, Martinez JM, Roque L, Coll T, Hervas R, Calvis C, Messeguer R, Mitjans F and Hernández JL. S100P antibody-mediated therapy as a new promising strategy for the treatment of pancreatic cancer. Oncogenesis 2014; 3: e92.
[40] Basu GD, Azorsa DO, Kiefer JA, Rojas AM, Tuzmen S, Barrett MT, Trent JM, Kallioniemi O and Mousses S. Functional evidence implicating S100P in prostate cancer progression. Int J Cancer 2008; 123: 330-339.
[41] Ge F, Wang C, Wang W and Wu B. S100P predicts prognosis and drug resistance in gastric cancer. Int J Biol Markers 2013; 28: e387-392.
[42] Cong Y, Cui Y, Wang S, Jiang L, Cao J, Zhu S, Birkin E, Lane J, Ruge F, Jiang WG and Qiao G. Calcium-binding protein S100P promotes tumor progression but enhances chemosensitivity in breast cancer. Front Oncol 2020; 10: 566302.
[43] Shimizu S, Yoshida T, Tsujioka M and Arakawa S. Autophagic cell death and cancer. Int J Mol Sci 2014; 15: 3145-3153.
[44] Li X, Zhou Y, Li Y, Yang L, Ma Y, Peng X, Yang S, Liu J and Li H. Autophagy: a novel mechanism of chemoresistance in cancers. Biomed Pharmacother 2019; 119: 109415.
[45] Yu Y, Cao L, Yang L, Kang R, Lotze M and Tang D. microRNA 30A promotes autophagy in response to cancer therapy. Autophagy 2012; 8: 853-855.
[46] Duffy MJ, Synnott NC, O'Grady S and Crown J. Targeting p53 for the treatment of cancer. Semin Cancer Biol 2022; 79: 58-67.
[47] Feng Z, Zhang H, Levine AJ and Jin S. The coordinate regulation of the p53 and mTOR pathways in cells. Proc Natl Acad Sci U S A 2005; 102: 8204-8209.
[48] Jones RG, Plas DR, Kubek S, Buzzai M, Mu J, Xu Y, Birnbaum MJ and Thompson CB. AMP-activated protein kinase induces a p53-dependent metabolic checkpoint. Mol Cell 2005; 18: 283-293.
[49] He C and Klionsky DJ. Regulation mechanisms and signaling pathways of autophagy. Annu Rev Genet 2009; 43: 67-93.
[50] Wang Y, Liu Z, Shu S, Cai J, Tang C and Dong Z. AMPK/mTOR signaling in autophagy regulation during cisplatin-induced acute kidney injury. Front Physiol 2020; 11: 619730.

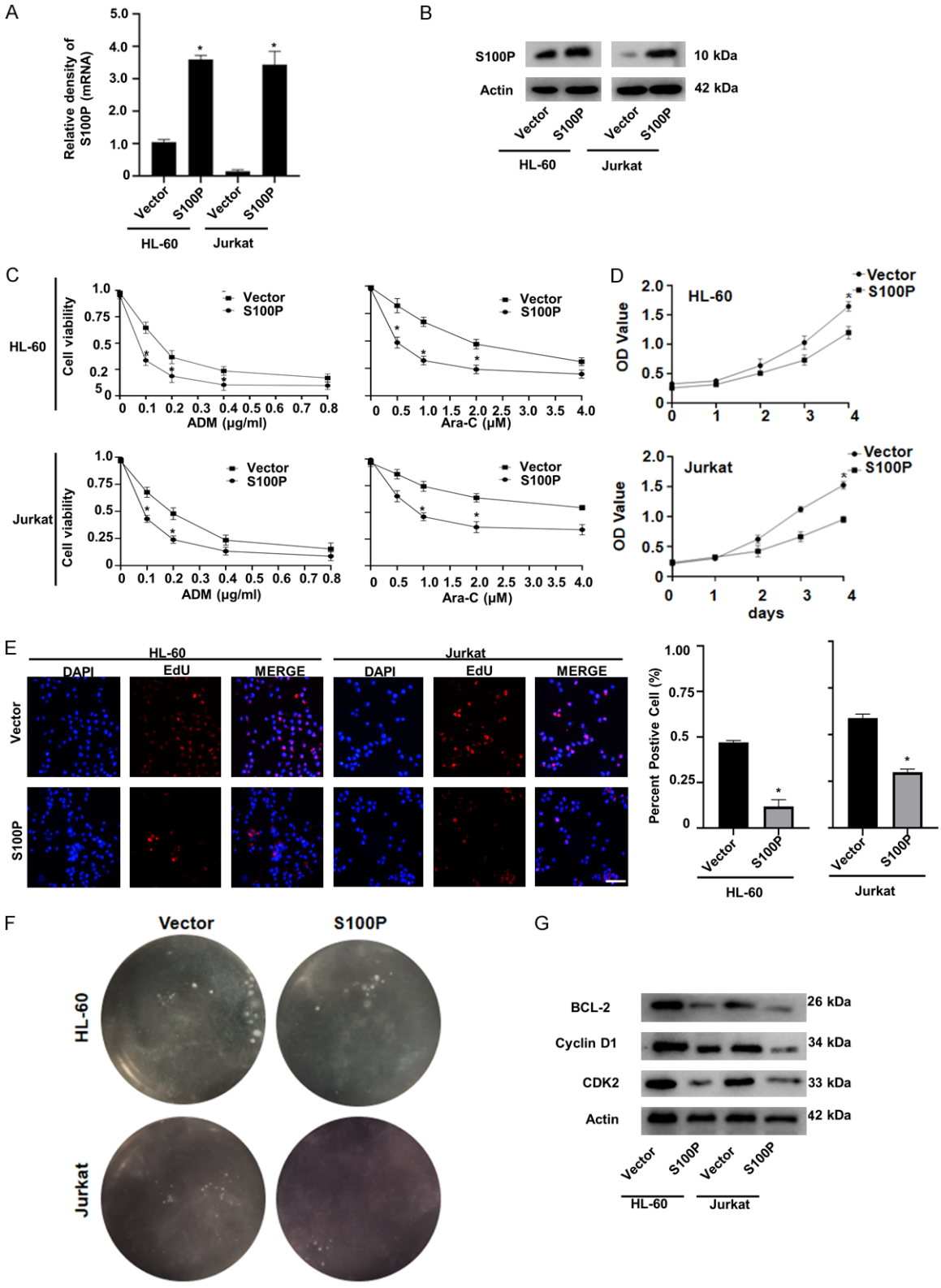

Figure S1. Upregulated S100P decreased leukemia cells proliferation and chemosensitivity. A, B. QRT-PCR and western blot analysis confirmed the up-regulation of S100P in HL-60 and Jurkat cells treated with S100P vector gene transfection. *P<0.05 vs. vector group; C. Upregulated S100P expression increased the sensitivity of leukemia cells to anti-cancer drug. Upregulated S100P by gene transfection in HL-60 or Jurkat cells and then treated with

ADM and Ara-C at the indicated doses for 24 h and 48 h respectively. Cell viability was assayed using a CCK-8 kit (n=3, *P<0.05 vs. vector group); D. Upregulated S100P inhibited the proliferation of HL-60 and Jurkat cells. HL-60 and Jurkat cells were transfected with S100P vector or empty vector and then cultured for 4 days. OD value was assayed using a CCK-8 kit for every day (n=3, *P<0.05 vs. vector group); E. EdU assays were performed and analyzed. Representative EdU analysis of cell proliferation in vector or S100P overexpression HL-60 or Jurkat cells. DAPI (blue) was used to stain nucleus and EdU (red) showed the incorporated cells. *P*-values have been calculated using paired Student's t-test. Scale bar: 50 μm (n=3, *P<0.05 vs. vector group); F. Upregulated S100P suppressed the colony formation of HL-60 and Jurkat cells. HL-60 and Jurkat cells were transfected with S100P vector or empty vector and then soft agarose colony formation were performed; G. Upregulated S100P contributed to reduction of Cyclin D1, CDK2 and Bcl-2. HL-60 and Jurkat cells were transfected with S100P vector or empty vector and then Cyclin D1, CDK2 and Bcl-2 levels were assayed by western blot.

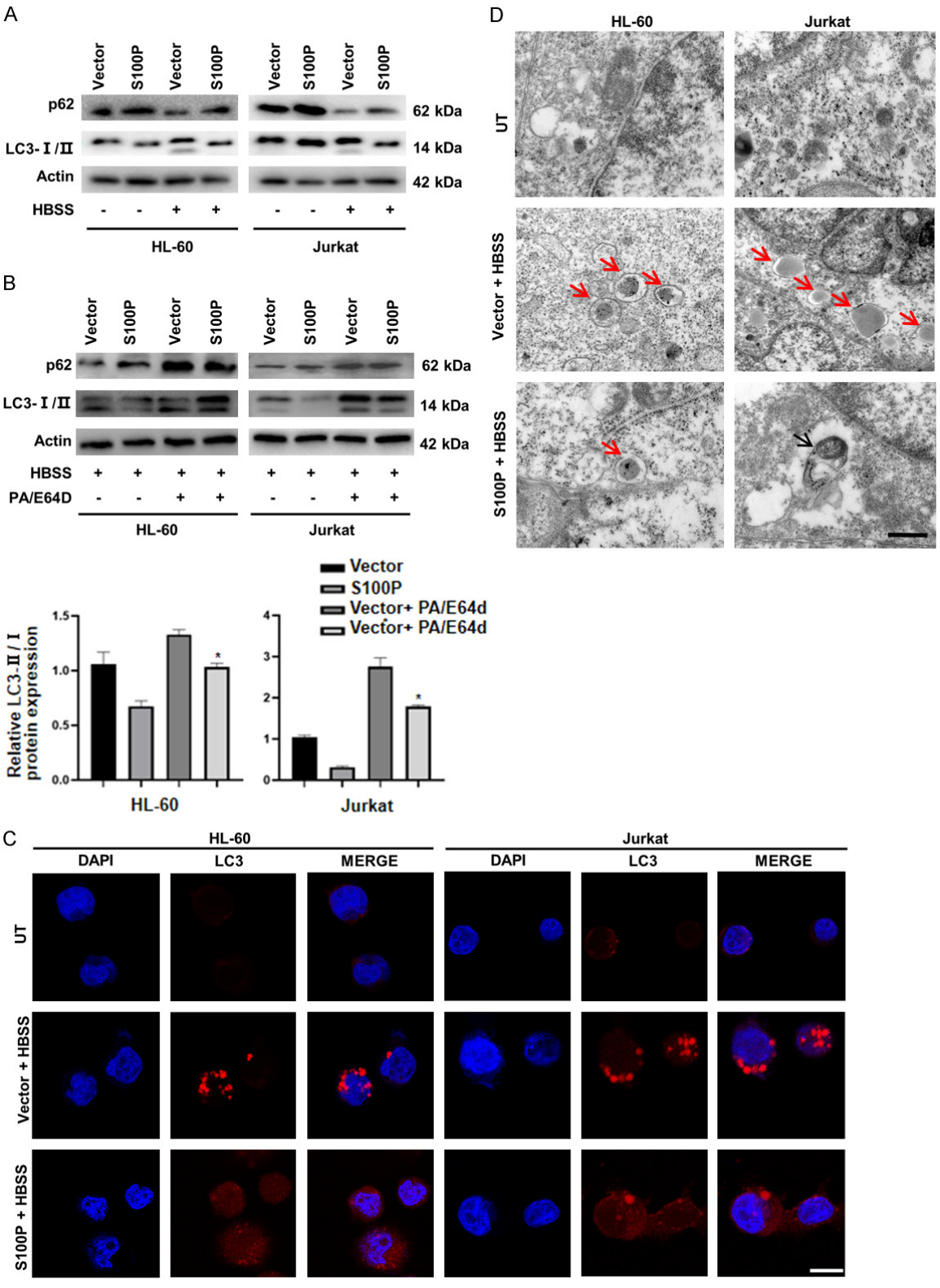

Figure S2. Upregulated S100P decreased HBSS-induced autophagy in leukemia cells. A. HL-60 and Jurkat cells were transfected with S100P vector or empty vector and then starved by HBSS for 2 h. LC3-I/II and p62 levels were assayed by western blot; B. HL-60 and Jurkat cells were transfected with S100P vector or empty vector and then pre-treated with pepstatin A (PA, 10 μM) and E64d (10 μM) for 1 h. Cells were subsequently treated for 2 h with HBSS in continuous presence or absence PA/E64d inhibitors. LC3-I/II and p62 levels were assayed by western blot (n=3, *P<0.05 vs. vector group); C. Ultrastructural features in HL-60 and Jurkat cells transfected with S100P vector or

empty vector after 2 h treatment of HBSS. More autophagolysosomes were seen in empty vector plus HBSS-treated cells than in cells treated with S100P vector plus HBSS. Red arrows indicated autophagolysosomes. Black arrows indicated autophagosomes. Scale bar: 500 nm; D. HL-60 and Jurkat cells were transfected with S100P vector or empty vector and then starved by HBSS for 2 h and then immunostained with LC3B-specifc antibody (red) and DAPI (blue). Scale bar: 10 μm.

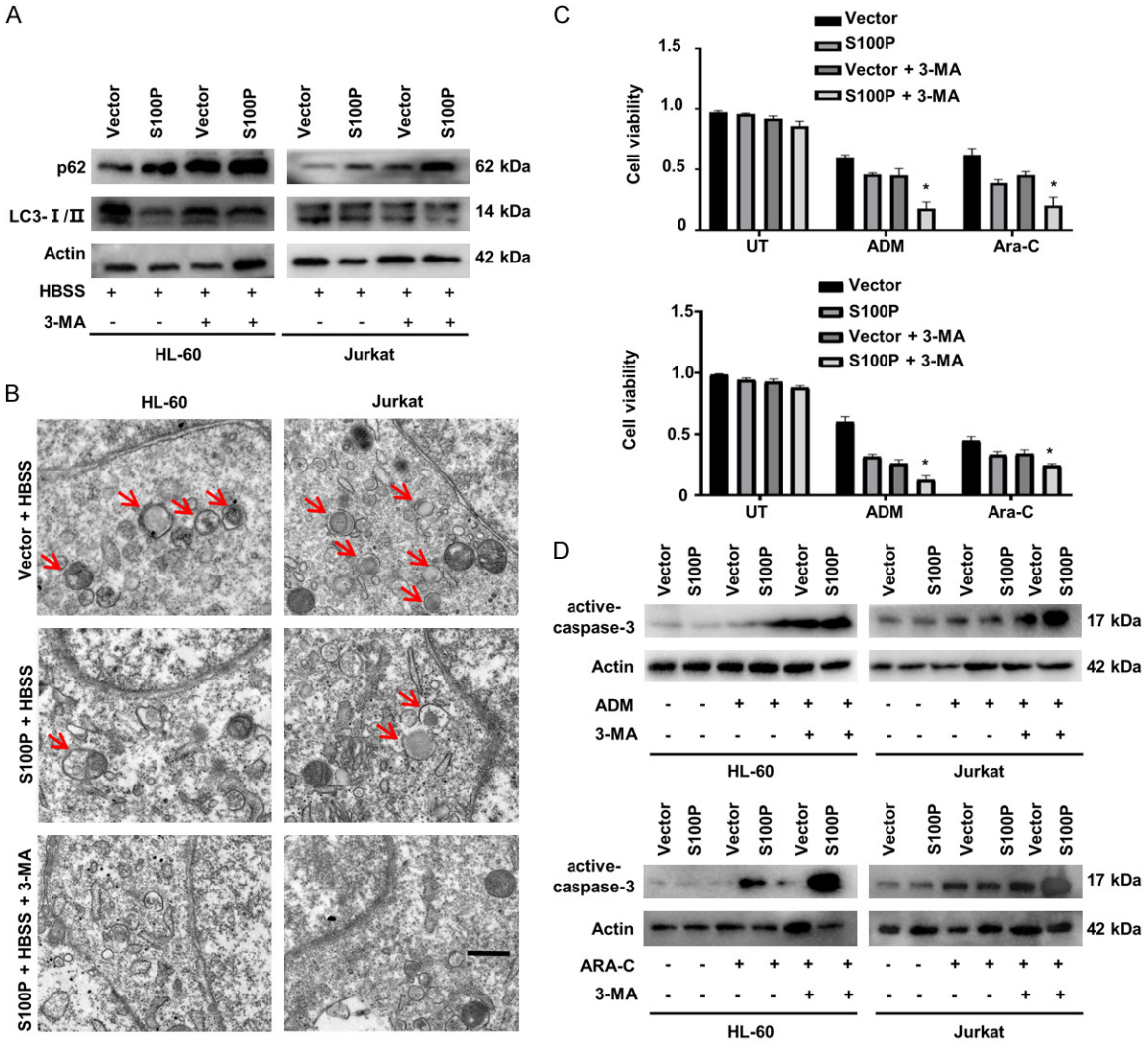

Figure S3. Inhibition of autophagy increased upregulated S100P-enhanced chemosensitivity. A, B. Inhibitor of autophagy blocked the initiation of autophagy. Analysis of LC3 and p62 expressions by western blot and number of autophagosomes by electron microscopy in the presence or absence of 3-MA (10 mM) treatment for 1 h in S100P vector or empty vector cells, followed by treatment with HBSS for 2 h. Red arrows indicate autophagolysosomes. Scale bar: 500 nm; C. Inhibition of autophagy increased upregulated S100P-enhanced chemosensitivity. HL-60 and Jurkat cells were transfected with S100P vector or empty vector and then pre-treated with 3-MA (10 mM) for 1 h. Cells were subsequently treated for 24 h with ADM (0.2 μg/ml) and 48 h Ara-C (4 μM) respectively, then cell viability was assayed using a CCK-8 kit (n=3, *P<0.05 vs. S100P group); D. Inhibition of autophagy reversed upregulated S100P-enhanced cells death. HL-60 and Jurkat cells were transfected with S100P or empty vector and then pre-treated for 1 h with 3-MA (10 mM) as indicated. Cells were subsequently treated for 24 h with ADM (0.2 μg/ml), then active caspase-3 levels were assayed by western blot.

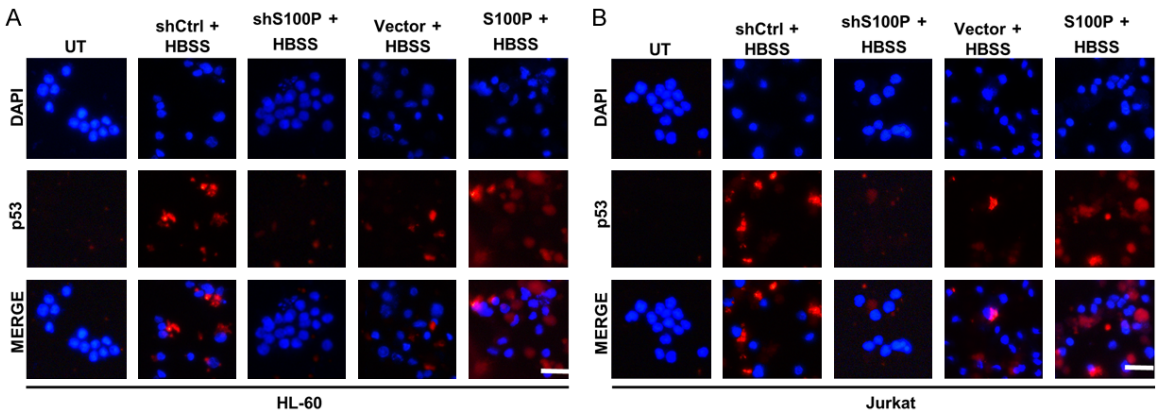

Figure S4. Endogenous S100P regulated p53 cytoplasmic translocation. A. S100P-deficient HL-60 cells and S100P-overexpression HL-60 cells were starved by HBSS for 2 h, and then immunostained with p53-specific antibody (red) and DAPI (blue). Scale bar: 10 μm; B. S100P-deficient Jurkat cells and S100P-overexpression Jurkat cells were starved by HBSS for 2 h, and then immunostained with p53-specific antibody (red) and DAPI (blue). Scale bar: 10 μm.